Synthesis and Design of Direct-Coupled Rectangular Waveguide Filters with Arbitrary Inverter Sequence

Qianqian Wang and Jens Bornemann
Department of Electrical and Computer Engineering
University of Victoria
Victoria, BC, Canada

***Abstract*—A framework for the design of direct-coupled waveguide filters with both impedance and admittance inverters is presented. Combinations of sequences of four different inverter structures permit the use of both half-wave and quarter-wave resonators as well as the creation of transmission zeroes to the left and right of the passband. Many different and new filter designs are presented for common filter specifications and demonstrate the variety of possible design realizations. The difference between synthesized and optimized responses is explained. The coupled-integral equation technique is used for fast component design, and final performances are validated by the commercial software package μWaveWizard. Filter dimensions are provided.**

I. INTRODUCTION

Direct-coupled waveguide filters have been investigated for decades, e.g. [1], [2], and their synthesis using impedance/ admittance inverters and half-wavelength resonators is well documented [3]-[5]. Although filters with quarter-wavelength resonators have been presented as early as 1958 [6], the advantage of using alternating impedance and admittance inverters has been employed sparsely. Only recently has this principle been rediscovered for the design of printed-circuit filters [7]. Another variety of the direct-coupled waveguide filter is the use of so-called frequency-dependent inverters to introduce transmission zeros [8], [9].

This paper presents a framework for the synthesis and design of rectangular waveguide filters. It contains a variety of different inverters whose sequence is predetermined during the synthesis stage. Moreover, the method includes the generation of transmission zeroes below and above the passband and utilizes both half-wave and quarter-wave resonators and combinations thereof. Several new rectangular waveguide filter configurations are presented that become only possible by selecting the type of each individual inverter and specifying its length or thickness so that its width can be used for the synthesis process.

II. THEORY

Traditionally, the design procedure commences with filter specifications in terms of center frequency, bandwidth, return loss, attenuation requirements and dimensions of the input/output waveguides. For the work presented here, we obtain five resonators for a Ku-band filter at 15 GHz, 600 MHz bandwidth, 24 dB return loss and 30 dB attenuation at 14 GHz and 16 GHz. The Chebychev filter coefficients are obtained from [3] and determine the normalized inverter values as follows [3].

$$k_{01} = \frac{K_{01}}{Z_0} = \sqrt{\frac{\pi}{2}\frac{B}{g_0 g_1}} = \frac{J_{01}}{Y_0} = j_{01} \tag{1a}$$

$$k_{n,n+1} = \frac{K_{n,n+1}}{Z_0} = \frac{\pi}{2}\frac{B}{\sqrt{g_n g_{n+1}}} = \frac{J_{n,n+1}}{Y_0} = j_{n,n+1} \tag{1b}$$

$$k_{N,N+1} = \frac{K_{N,N+1}}{Z_0} = \sqrt{\frac{\pi}{2}\frac{B}{g_N g_{N+1}}} = \frac{J_{N,N+1}}{Y_0} = j_{N,N+1} \tag{1c}$$

B is the normalized bandwidth, g_n the filter coefficients and $k_{n,n+1}$, $j_{n,n+1}$ the normalized impedance or admittance inverters, respectively.

At this stage, the type of inverters and their sequence is selected. Fig. 1 shows inductive-iris (Fig. 1a), capacitive-iris (Fig. 1b) inverters as well as their equivalent-circuit representations with series and shunt reactances and line sections that adjust the overall transmission phase to ±π/2.

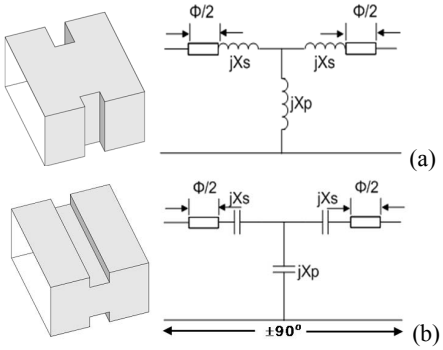

Figure 1. Inductive iris (a), capacitive iris (b) and their representations as impedance inverters.

For a specified thickness of the respective iris, its aperture is varied in a search algorithm until the inverter value computed from its scattering parameters

$$jX_s = \frac{(1-S_{21})^2 - S_{11}^2}{(1-S_{11})^2 - S_{21}^2} \tag{2a}$$

$$jX_p = \frac{2S_{21}}{(1-S_{11})^2 - S_{21}^2} \tag{2b}$$

978-1-4799-2225-3/14/$31.00 ©2014 IEEE

$$\phi = -\tan^{-1}\left(2X_p + X_s\right) - \tan^{-1} X_s \qquad (2c)$$

$$k = \left|\tan\left(\frac{\phi}{2} + \tan^{-1} X_s\right)\right| \qquad (2d)$$

equals that obtained from (1). In this work, the coupled-integral equation technique (CIET) is used to calculate the modal scattering matrices [10]. Note that with no loss of generality, we focus on symmetric inverters. Formulas for asymmetric inverters, in which the waveguides attached to an inverter have different cross sections, can be obtained, e.g., from [11].

If an inductive (Fig. 2a) or capacitive (Fig. 2b) admittance inverter is selected, then, instead of (2), the process uses (3).

$$jB_p = \frac{(1-S_{21})^2 - S_{11}^2}{(1+S_{11})^2 - S_{21}^2} \qquad (3a)$$

$$jB_s = \frac{2S_{21}}{(1+S_{11})^2 - S_{21}^2} \qquad (3b)$$

$$\phi = -\tan^{-1}\left(2B_s + B_p\right) - \tan^{-1} B_p \qquad (3c)$$

$$j = \left|\tan\left(\frac{\phi}{2} + \tan^{-1} B_p\right)\right| \qquad (3d)$$

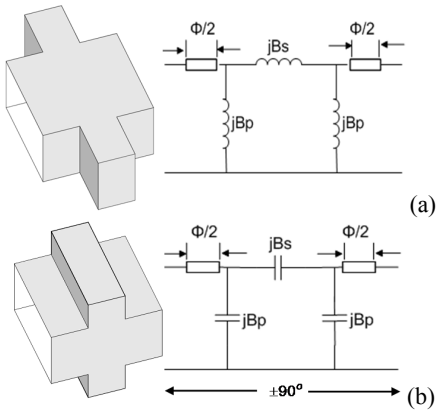

Figure 2. Inductive stub (a), capacitive stub (b) and their representations as admittance inverters.

Once all inverters have been determined, the resonator lengths are adjusted by

$$l_i = \frac{\lambda_{g0}}{2\pi}\left[\pi + \frac{1}{2}\left(\phi_{2,i} + \phi_{1,i+1}\right)\right] \qquad (4)$$

where λ_{g0} is the guided wavelength at midband frequency.

Note that (4) only applies if two subsequent inverters are either both impedance or both admittance inverters. In this case, the electrical length of the resonator between these inverters is a half-wavelength. If one inverter is of the impedance and the next of the admittance kind, then an additional inverter would be required. However, such a case can be adjusted by subtracting a transmission-line inverter, which is a quarter-wavelength section at midband frequency.

$$l_i = \frac{\lambda_{g0}}{2\pi}\left[\pi + \frac{1}{2}\left(\phi_{2,i} + \phi_{1,i+1}\right)\right] - \frac{\lambda_{g0}}{4} \qquad (6)$$

Thus such a scenario results in a quarter-wavelength resonator.

III. RESULTS

A. *Filters with half-wave resonators*

First we demonstrate the individual inverters of Fig. 1 and Fig. 2 as sole coupling sections in rectangular waveguide filters. Fig. 3a shows the response of the filter synthesized by inductive-iris inverters (Fig. 1a). It is observed that, since the inductive irises are separated by half a wavelength, the synthesized response satisfies the specifications and that a fine optimization of iris apertures and resonator lengths only achieves an equi-ripple performance (Fig. 3b). The commercial software package μWaveWizard is used in this work to validate individual filter designs. Note that the CIET algorithm includes an estimation of losses comprising of regular waveguide losses and unloaded-Q efficiencies based on a number of rectangular

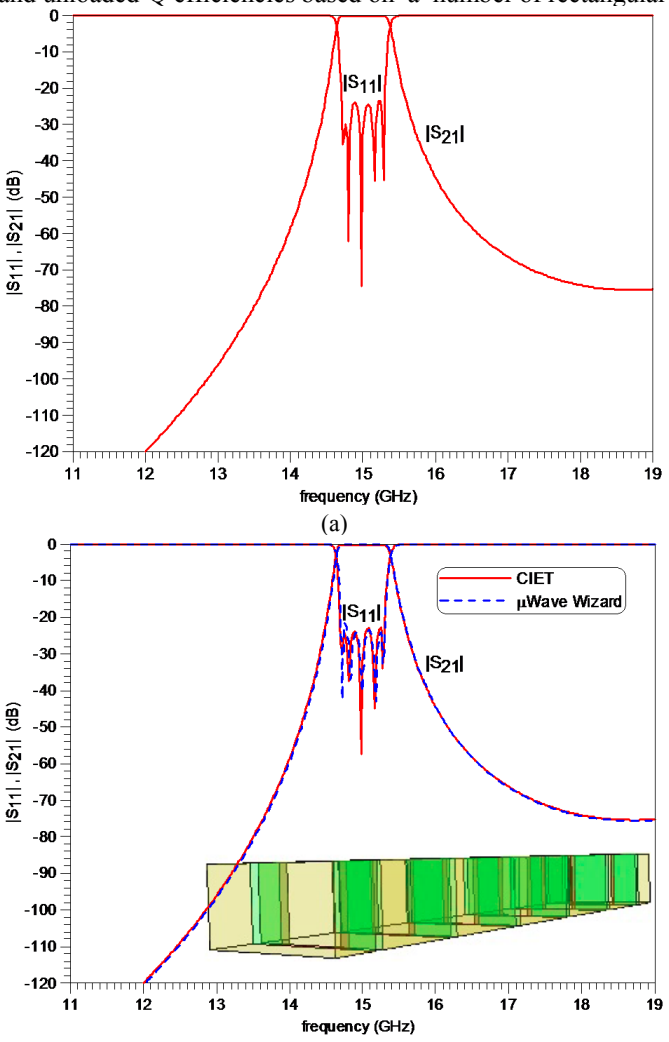

Figure 3. Response of all-inductive-iris filter according to Fig. 1a; synthesized (a), optimized (b).

Waveguide filter measurements. For the response in Fig. 3b, the insertion loss is estimated as 0.24 dB.

Fig. 4 shows a performance based on capacitive irises. Since capacitive irises 2, 3, 4 are synthesized with extremely small aperture widths (0.5 mm) for 6.063 mm thickness, insertion losses amount to 2.1 dB which explains the difference between CIET and µWaveWizard, the latter assuming lossless conditions. Note that capacitive-iris inverters provide a more symmetric filter response at the expense of a passband close to the waveguide's cutoff frequency due to the fact that propagation is principally possible in all irises and resonators.

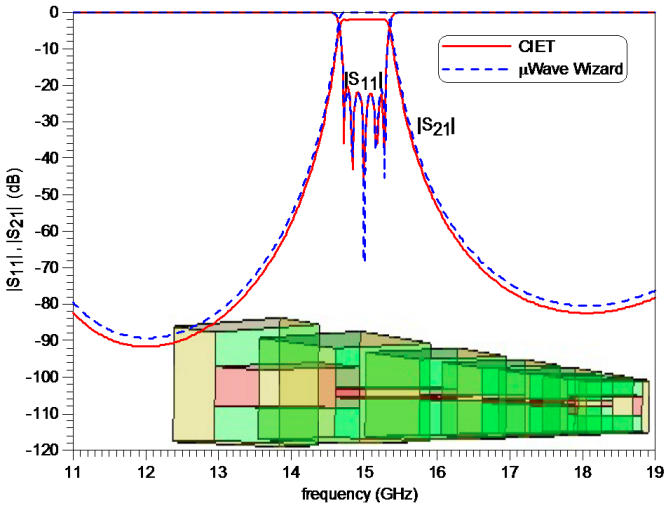

Figure 4. Response of optimized all-capacitive-iris filter according to Fig. 1b.

Fig. 5 depicts a synthesized (not optimized) design solely based on admittance inverters of Fig. 2a. Since the inductive stubs of 15.8 mm lengths permit many resonances, additional wide passbands are created to the left and right of the 15 GHz band. However, their ability to create transmission zeroes is demonstrated in Fig. 5 – a capability that will be exploited later.

The same applies to all-capacitive admittance inverters according to Fig. 2b. Compared to Fig. 5, the filter in Fig. 6 achieves the correct bandwidth with additional passbands moved down and up in frequency, thus providing a better response than shown in Fig. 5. Note that the generation of transmission zeroes is an agreement with [8].

The performance of a filter with a combination of capacitive-irises (irises 1 and 6) and inductive irises (irises 2 to 5) with half-wavelength resonators is depicted in Fig. 7. The filter characteristic is slightly more symmetric than with all-inductive irises (Fig. 3b) due to the effect of capacitive irises. This is a fair and realizable compromise between capacitive- and inductive-iris impedance inverters that produces an estimated insertion loss of 0.43 dB.

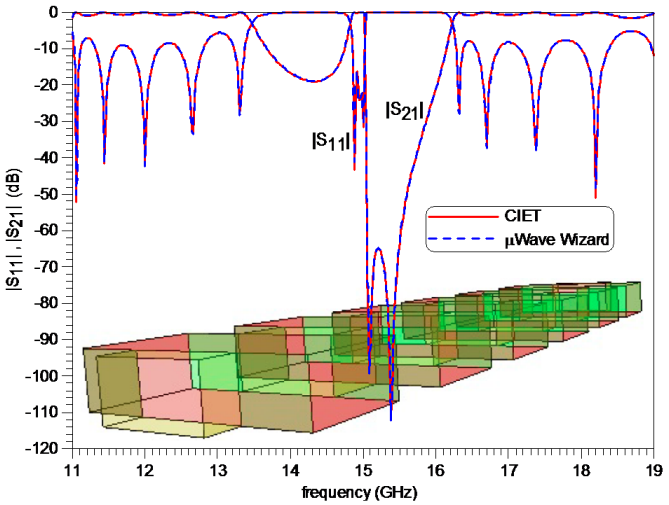

Figure 5. Response of synthesized all-inductive-stub filter according to Fig. 2a.

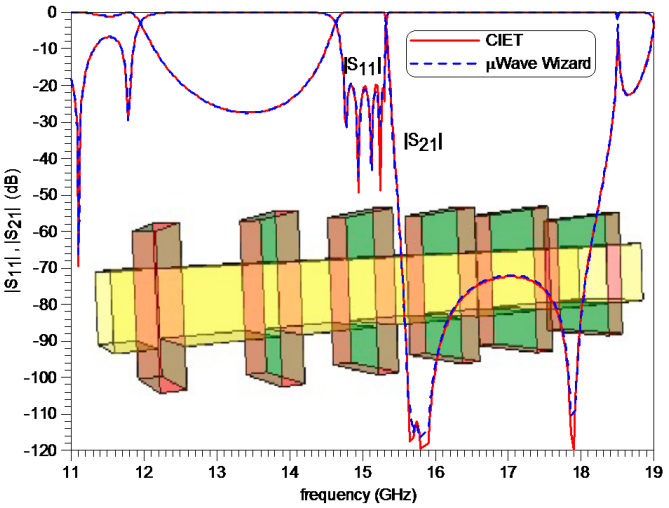

Figure 6. Response of optimized all-capacitive-stub filter according to Fig. 2b.

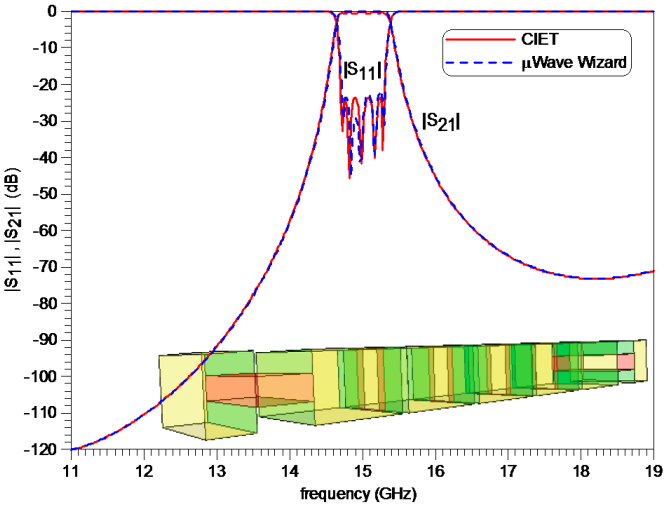

Figure 7. Response of optimized filter with two capacitive irises (Fig. 1b) and four inductive irises (Fig. 1b).

B. *Filters with half- and quarter-wave resonators*

As pointed out earlier, when stubs and irises are used as subsequent inverters, the electrical length of the resonator between them is chosen a quarter-wavelength. When admittance inverters are selected as first and last inverters, then this scenario addresses the use of frequency-dependent inverters, previously presented in [9]. With an inductive-iris length of 15.8 mm, a transmission zero is generated at 15.8 GHz (Fig. 8a). To move the transmission zero to the left at 13 GHz, the length of the inductive stubs is increased to 25.53 mm (Fig. 8b). The second transmission zero at 16.1 GHz is in agreement with observations in [9].

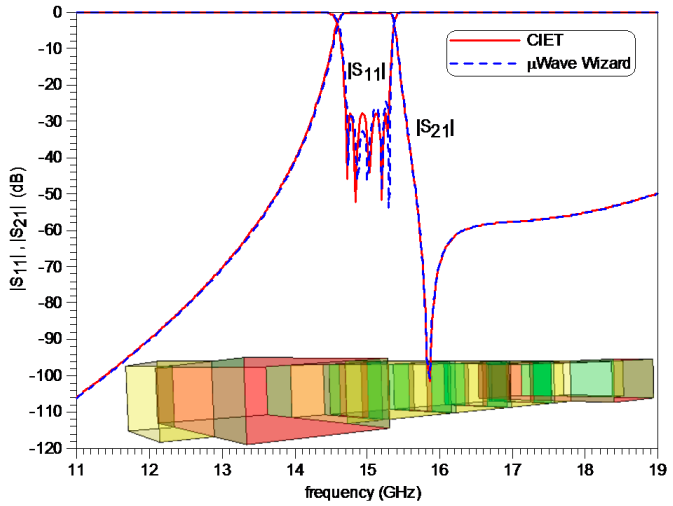

(a)

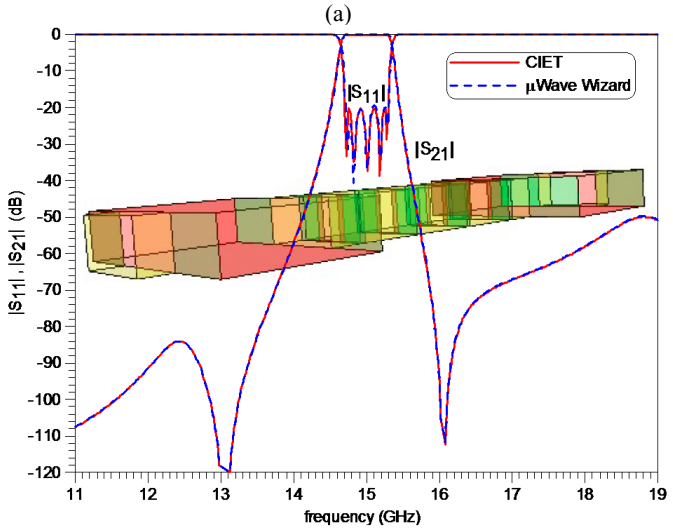

(b)

Figure 8. Responses of optimized inductive-iris filters with inductive stubs as first and last inverters; resonators 1 and 5 are quarter-wave resonators; stub lengths = 15.80 mm (a), 25.53 mm (b).

The filter in Fig. 9 has capacitive-stub admittance inverters as 2nd and 5th inverters, all other ones being inductive-iris impedance inverters. Consequently, only the center resonator is a half-wavelength long while all other ones are a quarter-wavelength. The two identical admittance inverters produce a transmission zero at 15.64 GHz. The insertion loss is estimated as 0.34 dB.

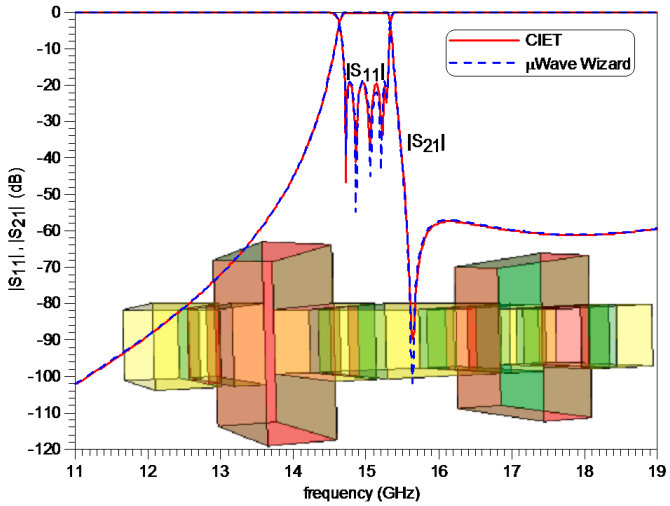

Figure 9. Response of optimized filter with four inductive irises and two capacitive stubs; only the center resonator is half-wave, all others are quarter-wavelength long.

C. *Filter with quarter-wave resonators*

Alternating impedance and admittance inverters produce filters with all quarter-wavelength resonators [6]. This is demonstrated in Fig. 10. In order to produce a symmetric filter, the number of resonators has been reduced to four. However, an asymmetric filter can be synthesized and designed if the filter order was to be maintained at five. Fig. 10a shows the synthesized response following the procedure outlined in Section II. When using mixed inverters with quarter-wavelength resonators, the synthesized response is acceptable (Fig. 10a) but normally fails to show the correct number of reflection zeros. This is due to the fact that inverters are much closer to each other than with half-wave resonators, e.g. Fig. 3a, and that they are influencing each other through the short resonator section. Thus further fine-optimization is usually required to satisfy specifications. Fig 10b demonstrates the result after optimization. The first and last capacitive-stub admittance inverters are identical while the center one is different. Thus two transmission zeros at 15.5 GHz and 17.76 GHz are created. These transmission zeros can be moved by changing the initial length of the capacitive-stub admittance inverters. The maximum insertion loss of this filter is estimated at 0.38 dB.

If a transmission zero to the left of the passband is desired, for instance as in Fig. 8b, then the first and last capacitive stubs in Fig. 10b can be replaced by inductive-stub admittance inverters. The final performance of such a filter after fine optimization is depicted in Fig. 11. It is observed that transmission zeros appear at 13.93 GHz, 15.56 GHz and 17.52 GHz. The maximum inband insertion loss is estimated as 0.29 dB.

Note that the dimensions (rounded to 1 µm) of all designs presented in this paper are depicted in Table I and Table II. Section widths are shown as a_n, section heights as b_n, and section lengths as l_n. Since all filters are symmetric, parameters are only shown up to the center filter section. All designs in Fig. 3 to Fig. 11 are verified by the commercial software package µWaveWizard.

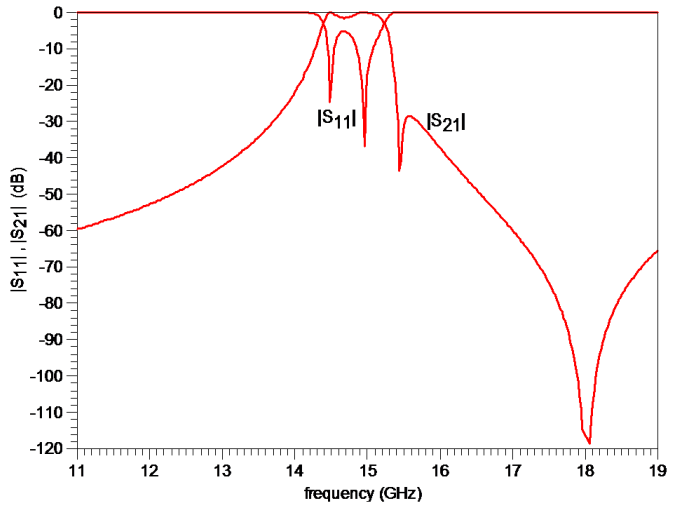

(a)

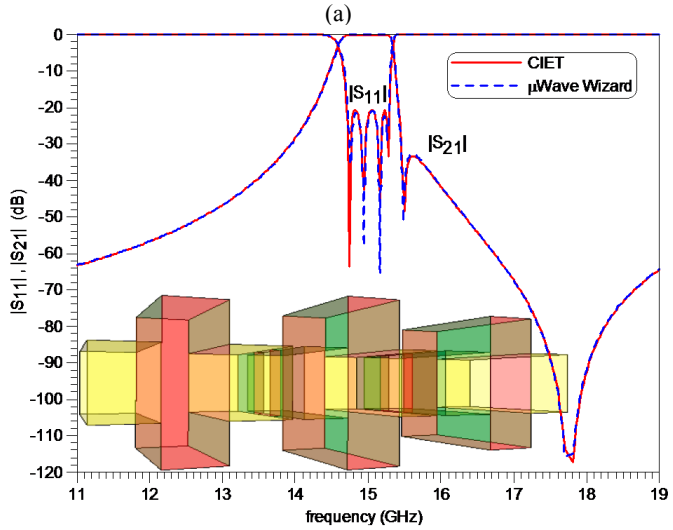

(b)

Figure 10. Response of four-pole all-quarter-wavelength resonator filter; synthesized (a), optimized (b).

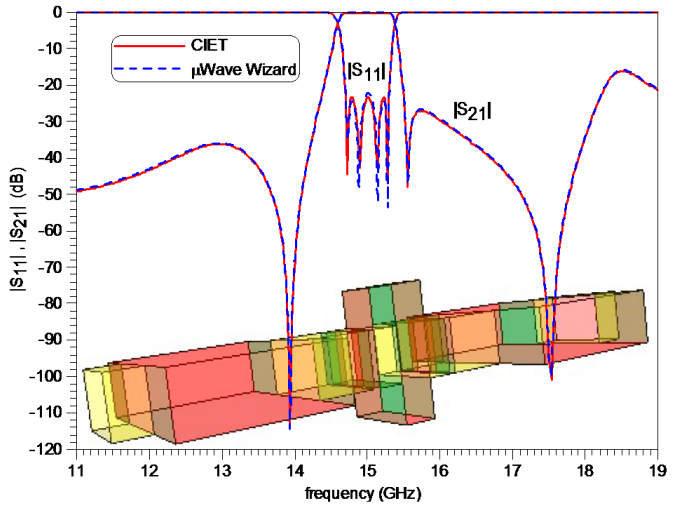

Figure 11. Response of four-pole all-quarter-wavelength resonator filter with inductive-stub admittance, inductive-iris impedance and capacitive-stub admittance inverters

TABLE I. DIMENSIONS OF FILTER DESIGNS (IN MM) SHOWN IN FIG. 3 TO FIG. 7.

	Fig. 3b	Fig. 4	Fig. 5	Fig. 6	Fig. 7
a_0	15.799	15.799	15.799	15.799	15.799
a_1	7.688	15.799	35.326	15.799	15.799
$a2$	15.799	15.799	15.799	15.799	15.799
a_3	4.996	15.799	36.254	15.799	5.131
a_4	15.799	15.799	15.799	15.799	15.799
a_5	4.485	15.799	36.347	15.799	4.477
a_6	15.799	15.799	15.799	15.799	15.799
b_0	7.899	7.899	7.899	7.899	7.899
b_1	7.899	2.913	7.899	16.507	2.964
b_2	7.899	7.899	7.899	7.899	7.899
b_3	7.899	0.832	7.899	18.475	7.899
b_4	7.899	7.899	7.899	7.899	7.899
b_5	7.899	0.569	7.899	18.704	7.899
b_6	7.899	7.899	7.899	7.899	7.899
l_0	5.000	5.000	5.000	5.000	5.000
l_1	1.000	6.063	15.800	3.145	6.421
l_2	10.533	12.806	9.298	12.192	12.053
l_3	1.000	6.063	15.800	3.145	1.000
l_4	11.793	12.887	8.178	10.968	11.758
l_5	1.000	6.063	15.800	3.145	1.000
l_6	11.938	12.900	8.058	10.805	11.943

TABLE II. DIMENSIONS OF FILTER DESIGNS (IN MM) SHOWN IN FIG. 8 TO FIG. 11.

	Fig. 8a	Fig. 8b	Fig. 9	Fig. 10b	Fig. 11
a_0	15.799	15.799	15.799	15.799	15.799
a_1	34.041	38.902	7.077	15.799	36.752
$a2$	15.799	15.799	15.799	15.799	15.799
a_3	6.035	5.539	15.799	4.874	5.410
a_4	15.799	15.799	15.799	15.799	15.799
a_5	4.593	4.400	4.209	15.799	15.799
a_6	15.799	15.799	15.799		
b_0	7.899	7.899	7.899	7.899	7.899
b_1	7.899	7.899	7.899	16.954	7.899
b_2	7.899	7.899	7.899	7.899	7.899
b_3	7.899	7.899	19.804	7.899	7.899
b_4	7.899	7.899	7.899	7.899	7.899
b_5	7.899	7.899	7.899	19.585	19.450
b_6	7.899	7.899	7.899		
l_0	5.000	5.000	5.000	5.000	5.000
l_1	15.800	25.527	1.000	5.000	22.489
l_2	5.397	5.836	2.658	5.098	8.785
l_3	1.000	1.000	6.000	1.0000	1.000
l_4	11.547	11.683	3.821	4.082	3.701
l_5	1.000	1.000	1.0000	5.000	5.010
l_6	11.944	12.002	12.121		

IV. CONCLUSIONS

A framework for the synthesis and design of direct-coupled rectangular waveguide filters with arbitrary inverter sequence is presented. The individual sequences of impedance and admittance inverters can result in all half-wavelength

resonators, all quarter-wavelength resonators or combinations thereof. Admittance stub inverters produce transmission zeros which can be located to the left or right of the passband. A previously published topic on frequency-dependent inverters is included in the synthesis, and the performance of such designs is shown to be equivalent, thus largely eliminating the optimization work of frequency-dependent inverters. All final performances are verified by comparison between the coupled-integral equation technique and the commercial software package μWaveWizard. Dimensions of all filter designs are provided.

ACKNOWLEDGEMENT

The authors acknowledge support for this work by the TELUS Research Grant in Wireless Communications.

REFERENCES

[1] S. B. Cohn, "Direct-coupled-resonator filters," Proc. IRE, vol. 45, pp. 187–196, Feb. 1957.

[2] R. Levy, "Theory of direct-coupled-cavity filters," IEEE Trans. Microwave Theory Tech., vol. 15, pp. 340–348, June 1967.

[3] G.L. Matthaei, L. Young, and E.M.T Jones, Microwave Filters, Impedance Matching Networks, and Coupling Structures, Artech House, Boston, 1980.

[4] Y.C. Shih and T. Itoh, "Computer-aided design of millimeter-wave E-plane filters," IEEE Trans. Microwave Theory Tech., vol. 31, pp. 135-142, Feb. 1983.

[5] J. Uher, J. Bornemann, and U. Rosenberg, Waveguide Components for Antenna Feed Systems. Theory and CAD, Artech House Inc., Norwood, MA, 1993.

[6] G.L. Matthaei, "Direct-coupled bandpass filters with $\lambda_0/4$ resonators," IRE Int. Conv. Record, vol. 6, pt. 1, pp. 98-111, 1958.

[7] S. Zhang and L. Zhu, "Synthesis method for even-order symmetrical Chebyshev bandpass filters with alternative J/K inverters and $\lambda/4$ resonators," IEEE Trans. Microwave Theory Tech., vol. 61, pp. 808-816, Feb. 2013.

[8] S. Amari and J. Bornemann, "Using frequency-dependent coupling to generate finite attenuation poles in direct-coupled resonator bandpass filters," IEEE Microw. Guided Wave Lett., vol. 9, pp. 404–406, Oct. 1999.

[9] J. Bornemann and J. Uher, "H-plane waveguide filters with E-plane dispersive inverters for high-power application," Proc. Antennas Electromagnetics (ANTEM), pp. 197–200, Ottawa, Canada, July 2004.

[10] J. Bornemann, U. Rosenberg, S. Amari, and R. Vahldieck, "Edge-conditioned vector basis functions for the analysis and optimization of rectangular waveguide dual-mode filters," IEEE MTT-S Int. Microwave Symp. Dig., pp. 1695-1698, Anaheim, USA, June 1999.

[11] J. Bornemann and J. Uher, "Synthesis of direct-coupled waveguide filters for integrated front-end applications", Proc. 3rd Int. Conf. Electromagnetics Aerospace Applications (ICEAA), pp. 151-154, Torino, Italy, Sep. 1993.